Feasibility of Bell tests with the W state

Amine Laghaout* and Gunnar Björk†

School of Information and Communication Technology, Royal Institute of Technology (KTH) Electrum 229, SE-164 40 Kista, Sweden

(Received 13 October 2009; published 11 March 2010)

The feasibility of Bell tests depends to a large extent on the tradeoff of difficulty between the preparation and the measurement of entangled systems. Polarization-entangled systems, though easy to measure, pose a relative challenge in their preparation. The opposite holds with entangled energy eigenstates for which the preparation is relatively straightforward. A way to perform measurements using a photodetector along the x, y, and z axes (in a Bloch sphere picture) on such Fock-state qubits shall be worked out, taking the W state as our entangled system. This will, by the same token, allow us to determine the minimum quantum efficiency required to perform a conclusive Bell test with the W energy eigenstate.

DOI: 10.1103/PhysRevA.81.033823 PACS number(s): 03.65.Ud

I. INTRODUCTION

From an experimental perspective, tests of nonlocality present a two-fold challenge: The first is the production of the entangled state and the second is its characterization. The choice of how to physically implement the entangled state, be it in terms of polarization, Fock states, or otherwise, should therefore take into account this tradeoff in difficulty between preparation and characterization. We shall, in this article, work with a W state as our entangled system. The choice of this state is motivated by the ubiquitous use of multiqubit systems in quantum information [1], where the W state offers the added advantage that entanglement of two of its qubits persists even if the third mode suffers decoherence [2,3]. We shall express it in Fock space as

$$|W\rangle = \frac{1}{\sqrt{3}}(|100\rangle + |010\rangle + |001\rangle). \tag{1}$$

We note that this is a special case of the single photon, n mode, W state, for which an "all-versus-nothing" test of local realism was recently proposed (with the predicted result being a violation of local realism) [4]. The preparation of this three-mode, single-photon state can be achieved by feeding a single photon into two consecutive beam splitters with reflectivities of $\frac{1}{3}$ and $\frac{1}{2}$, respectively. Had the W state consisted of polarization qubits instead, its preparation will be significantly more difficult [5]. Similarly, other proposals of Bell tests of W states trade a relatively simple detection for a complicated state preparation [6]. Given the relative ease with which the W can be prepared in terms of Fock states, it then remains to devise a way to characterize its entangled qubits. The first goal of this article is to work out a way to project qubits onto both the z and x axes of the Bloch sphere, where in terms of Fock states

$$\begin{aligned} z^- &= |0\rangle, \quad z^+ = |1\rangle, \\ x^\pm &= \frac{1}{\sqrt{2}}(|0\rangle \pm |1\rangle). \end{aligned} \tag{2}$$

Projection onto the z basis is thus relatively easy as it corresponds to a zero or one-photon number measurement outcome from an avalanche photo diode. An x and y-basis projection in this basis using a photo diode is nontrivial.

The need to project the qubits onto (in this case) two orthonormal axes of the Bloch sphere stems from the tripartite Bell inequality of Cabello [7] we seek to violate

$$\begin{aligned} 0 \leqslant 1 + P(z_i = -1, z_j = -1) - P(z_i = -1, x_j \neq x_k) \\ - P(x_i \neq x_k, z_j = -1) - P(x_i = x_j = x_k) \leqslant 1. \end{aligned} \tag{3}$$

(Here, we added unity to the original inequality for convenience.) The indices ijk are used in two different ways. For the first and fourth terms, the probabilities are summed over all permutations of ijk. For the middle two terms, however, ijk refer to a specific combination and are therefore fixed. In either case, i, j, and k indicate distinct modes. The eigenvectors of $\mathbf{z}$ and $\mathbf{x}$ are given in Eq. (2) and the associated eigenvalues assumed when deriving Eq. (3) are ± 1.

Theoretically, the inequality is violated by the W state by a factor of 1.25. (Any local realistic model will predict a value in the range 0 to 1, while the W state will achieve the value 1.25 [7].) However, because of experimental imperfections, this factor may be significantly less, or even below unity, thereby rendering local and quantum predictions undistinguishable in the laboratory. The second goal of this article is thus to quantify the minimum quantum efficiencies that allow for a violation of Eq. (3). An analysis for the violation of bipartite local realistic theories, much along the same lines, was undertaken by Wieśniak and Żukowski [8].

The article outline is as follows. In Sec. II we shall work out a way to perform measurements of a single qubit in the three maximally noncommuting bases (sometimes referred to as a set of mutually unbiased bases). Our proposed technique bears some similarity to single-photon homodyning, except that we are interested not in a quadrature amplitude [9], but in the discrete x-basis projection. In Sec. III we shall extend the discussion to the tripartite W state and derive projection probabilities as functions of experimental parameters. Finally in Sec. IV, Bell's inequality will be numerically analyzed to delimit the range of experimental imperfections that permit a validation of the inequality.

*laghaout@kth.se
†gunnarb@ele.kth.se

II. EXPERIMENTAL SELECTION OF BASES

A. Detection probabilities for a single qubit

Since photodetection is presently the only measurement tool at our disposal at the single photon level, the probability of detecting a given number of photons is the only statistic that can be gathered. The projection of a qubit on some axis of the Bloch sphere has then to be somehow related to the probability of detection or no-detection of photons. A generic qubit can be written $|\psi_0\rangle = \sqrt{p}|0\rangle + e^{i\Phi}\sqrt{1-p}|1\rangle$ (where $0 \leqslant p \leqslant 1$). Both the probability p and the quantum phase Φ are, in general, unknown, *a priori*, but as was shown [10,11] a mixing of the qubit with a coherent state $|\alpha\rangle$ with phase θ will generate beats in terms of $|\Phi - \theta|$, which will allow us to extract information as to the initial orientation of the qubit (Fig. 1). Let us explore this idea, applying a setup that is similar to that used to characterize squeezed states, namely an unbalanced homodyne measurement [10,12–14].

For example, the probability of detecting no photons at detector A in Fig. 1 is obtained by summing the projection $\langle 0, m, k|\psi_{\text{out}}\rangle$ over all ancillary modes, labeled k and m

$$\begin{aligned} P(n=0) &= \sum_{m=0}^{\infty}\sum_{k=0}^{\infty} |\langle 0, m, k|\psi_{\text{out}}\rangle|^2 \\ &= e^{-\beta^2\eta^2}[p + (1-p)(1 - t^2\eta^2 + t^2\beta^2\eta^4) \\ &\quad + 2\sqrt{p(1-p)}\beta t\eta^2 \cos(\Phi - \theta)], \end{aligned} \tag{4}$$

where $t(r)$ is the beam splitter transmittivity (reflectivity) where $r = (1-t^2)^{1/2}$ and we can, without any loss of generality, assume that both are real and positive, $\beta = |\alpha|r$, θ is the phase angle of the coherent field as $\alpha = |\alpha|e^{i\theta}$, and η^2 is the detector quantum efficiency.

In an experimental setting, laser phase diffusion will make it difficult to keep the phase-difference $\Phi - \theta$ constant over time if the qubit and the laser come from independent sources and propagate along independent paths to the mixing beam splitter. However, by using the polarization degree of freedom and making the qubit and the local oscillator copropagate, but have orthogonal polarizations this stability problem can be solved, as suggested in Ref. [11] and demonstrated in Ref. [15].

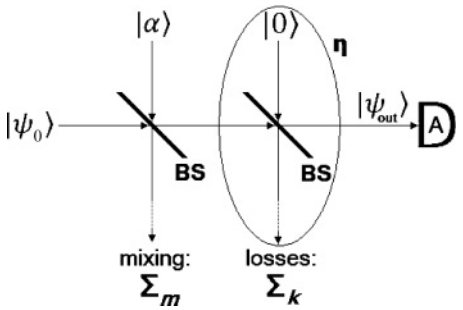

FIG. 1. Setup of the four-port unbalanced homodyne measurement that is used to create beats between the Fock-state qubit and the coherent field. The second beam splitter is only shown to model losses (since detectors in the real world are inevitably imperfect) and is not present in the actual setup. The detector A in this theoretical depiction is therefore assumed to be ideal.

B. Characterization of a qubit

Now that we can compute the probability of detecting any given number of photons, we need to relate that probability to the direction the input qubit $|\psi_0\rangle$ has in the Bloch sphere. That is, we need to know how to set up the experimental parameters to project the qubit in either the z or x basis.

The measurement of z projections is straightforward since the z basis is the *pointer* basis in which the meter-environment interaction Hamiltonian is diagonal [16]. It suffices to remove the first beam splitter from Fig. 1 and check whether a photon is detected (z^+) or not (z^-). In the x basis, however, photodetection only allows approximate projections and the homodyne setup described previously is then needed. To this end we set $t \to 1$ and $\alpha \to \infty$ in such a way that $|\alpha|r = \beta = 1$. Plugging all these parameters into expression (4) and assuming an ideal quantum efficiency, we obtain $P(n=0)$ as a function of Φ (solid line in Fig. 2).

C. Rescaling of projective probabilities in the x and y bases

The method devised previously to conduct measurements in the x basis is *a priori* unsatisfactory since it calls upon approximate projectors. In this instance, we are only "sure" by about 74% that we have x^- if no photon is detected.

Going back to Fig. 2, we see that if only a rescaling of the $P(n=0)$ function can be legitimized, we can "stretch" the 74% certainty in measuring x^- to a 100% certainty, thereby allowing for a confident identification of the x projection of the state. The way to legitimize such a rescaling is to check that the experimental function $P_{\text{expt}} = P(n=0)$ obtained in Eq. (4) is strictly proportional to its theoretical counterpart $P_{\text{theor}} = |\langle x^{\pm}|\psi_0\rangle|^2$. This turns out to be indeed the case under one crucial assumption, namely that the quantum efficiency be close to unity, that is, $\eta \approx 1$. In this case

$$P_{\text{theor}}(x^{\pm}) = \tfrac{1}{2}[1 \pm 2\sqrt{p(1-p)}\cos\Phi], \tag{5}$$

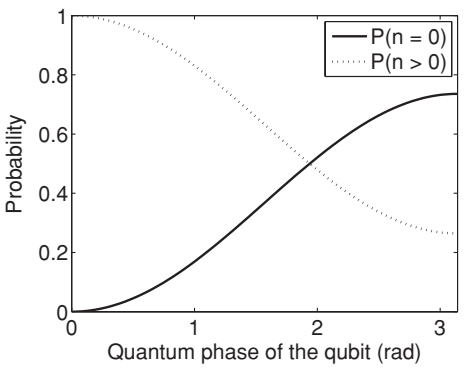

FIG. 2. Probabilities for detection $P(n>0)$ and no-detection $P(n=0)$ as functions of the quantum phase Φ of a single qubit. The phase for the coherent field is fixed at $\theta = \pi$. A horizontally symmetric plot is obtained for $\theta = 0$.

and

$$P_{\text{expt}}(x^{\pm}) = e^{-1}[1 \pm 2\sqrt{p(1-p)}\cos\Phi], \tag{6}$$

where we chose the additional parameters as $t \approx 1$ and $\beta = 1$. Hence

$$P_{\text{theor}}(x^{\pm}) = \kappa P_{\text{expt}}(x^{\pm}) \; \forall \, |\psi_0\rangle \Rightarrow \kappa = \frac{e}{2}. \tag{7}$$

A slightly more sophisticated analysis, involving Eq. (4) and the fact that the sum of the x^+ and x^- projection probabilities for any qubit state should equal unity, gives the proportionality factor

$$\kappa(\eta) = \frac{e^{\eta^2}}{2 - \eta^2 + \eta^4}, \tag{8}$$

for $t \approx 1$ and $\beta = 1$. The proportionality factor $\kappa(\eta)$ will subsequently be used as a multiplicative constant to rescale P_{expt} to become the estimated probability of a projection onto the x basis. The factor will ensure that for any quantum efficiency, the sum of the two possible probabilities for any orthogonal qubit projection is normalized to unity. For example, the probability of an x^- projection is given by $\kappa(\eta)P(n = 0 \mid t \to 1, \beta = 1, \theta = \pi)$ or if one wants to associate clicks rather than no-clicks to such a projection $\kappa(\eta)[1 - P(n \geqslant 1 \mid t \to 1, \beta = 1, \theta = \pi)]$. Similarly, for an x^+ measurement, we shall use $\kappa(\eta)P(n = 0 \mid t \to 1, \beta = 1, \theta = 0)$. One can similarly show that a y^+ projection is accomplished through the setting $\kappa(\eta)P(n = 0 \mid t \to 1, \beta = 1, \theta = \pi/2)$ and a y^- projection through $\kappa(\eta)P(n = 0 \mid t \to 1, \beta = 1, \theta = 3\pi/2)$. With this scaling, our homodyne scheme is proven to perform approximate projective measurements onto the x or y basis, provided the quantum efficiency is close to unity. Just how close η has to be to unity shall be computed numerically in the next section. Before doing so, we shall first investigate the projectors' behavior under loss.

The z-projection probabilities, being based in a straightforward photodetection, will have the following values as a function of the detector quantum efficiency η^2

$$P(z = 1|z^+) = \eta^2, \tag{9}$$

$$P(z = -1|z^+) = 1 - \eta^2, \tag{10}$$

$$P(z = 1|z^-) = 0, \quad \text{and} \tag{11}$$

$$P(z = -1|z^-) = 1, \tag{12}$$

where $P(z = 1|z^+)$ is the probability of the projection result $z = 1$, given that the measured state is z^+. These probabilities assume that the detector dark count rate is negligible.

The corresponding results for the x projector when $\beta = 1$, $t \to 1$, and $p = 1/2$ (the latter which corresponds to the x^+ and x^- states) is obtained from Eq. (4), rescaled by the factor $\kappa(\eta)$ as explained previously

$$\begin{aligned} P(x = 1|x^+) &= P(x = -1|x^-) \\ &= \kappa(\eta)P(n = 0 \mid t \to 1, \beta = 1, \Phi - \theta = 0) \\ &= \frac{1}{2}\left(1 + \frac{2\eta^2}{2 - \eta^2 + \eta^4}\right), \quad \text{and} \end{aligned} \tag{13}$$

$$\begin{aligned} P(x = 1|x^-) &= P(x = -1|x^+) \\ &= \kappa(\eta)P(n = 0 \mid t \to 1, \beta = 1, \Phi - \theta = \pi) \\ &= \frac{1}{2}\left(1 - \frac{2\eta^2}{2 - \eta^2 + \eta^4}\right). \end{aligned} \tag{14}$$

We see that just as in the case with the z-basis projectors, the projection errors grow with decreasing detector quantum efficiency, but whereas there is an asymmetry between the detection of the z^+ and z^- states, the situation is symmetric for the x basis. As the quantum efficiency goes down, the probability of the correct projections $P(x = 1|x^+) = P(x = -1|x^-)$ decreases and the probability of the erroneous projections $P(x = -1|x^+) = P(x = 1|x^-)$ increase. When $\eta = 0$ both projections are completely random, as expected.

III. EXTENSION TO THE W STATE

We have so far only dealt with the characterization of individual qubits. The extension to the W simply appends the apparatus depicted in Fig. 1 to each of the three modes (Fig. 3). The initial state is then $|W\rangle \otimes |\alpha_1\rangle \otimes |\alpha_2\rangle \otimes |\alpha_3\rangle$ and the probability of detecting n_i photons in the ith mode is

$$\begin{aligned} P(n_1, n_2, n_3) &= \sum_{k,m}^{\infty} |\langle n_1 n_2 n_3, m_1 m_2 m_3, k_1 k_2 k_3 | \psi_{\text{out}} \rangle|^2 \\ &= \frac{1}{3} e^{-\beta_1^2 \eta_1^2} \frac{(\beta_1 \eta_1)^{2n_1}}{n_1!} e^{-\beta_2^2 \eta_2^2} \frac{(\beta_2 \eta_2)^{2n_2}}{n_2!} e^{-\beta_3^2 \eta_1^3} \frac{(\beta_3 \eta_3)^{2n_3}}{n_3!} \Bigg[3 + t_1^2 \beta_1^2 \eta_1^4 - t_1^2 \eta_1^2 + t_2^2 \beta_2^2 \eta_2^4 \\ &\quad - t_2^2 \eta_2^2 + t_3^2 \beta_3^2 \eta_3^4 - t_3^2 \eta_3^2 + \frac{t_1^2}{\beta_1^2} n_1^2 - 2 t_1^2 \eta_1^2 n_1 + \frac{t_2^2}{\beta_2^2} n_2^2 - 2 t_2^2 \eta_2^2 n_2 + \frac{t_3^2}{\beta_3^2} n_3^2 - 2 t_3^2 \eta_3^2 n_3 \\ &\quad + 2\cos(\theta_1 - \theta_2) \left(\beta_1 t_1 \eta_1^2 \beta_2 t_2 \eta_2^2 - \beta_1 t_1 \eta_1^2 \frac{t_2}{\beta_2} n_2 - \beta_2 t_2 \eta_2^2 \frac{t_1}{\beta_1} n_1 + \frac{t_1 t_2}{\beta_1 \beta_2} n_1 n_2 \right) \\ &\quad + 2\cos(\theta_1 - \theta_3) \left(\beta_1 t_1 \eta_1^2 \beta_3 t_3 \eta_3^2 - \beta_1 t_1 \eta_1^2 \frac{t_3}{\beta_3} n_3 - \beta_3 t_3 \eta_3^2 \frac{t_1}{\beta_1} n_1 + \frac{t_1 t_3}{\beta_1 \beta_3} n_1 n_3 \right) \\ &\quad + 2\cos(\theta_2 - \theta_3) \left(\beta_2 t_2 \eta_2^2 \beta_3 t_3 \eta_3^2 - \beta_2 t_2 \eta_2^2 \frac{t_3}{\beta_3} n_3 - \beta_3 t_3 \eta_3^2 \frac{t_2}{\beta_2} n_2 + \frac{t_2 t_3}{\beta_2 \beta_3} n_2 n_3 \right) \Bigg]. \end{aligned} \tag{15}$$

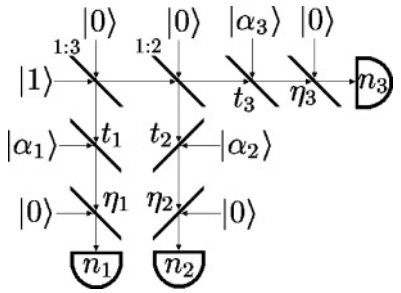

FIG. 3. Overall experimental setup for measuring the state of the W in different bases. Note that the local oscillator states (α_1, α_2, and α_3) in an experimental setup can be generated by splitting the output of single laser into three modes, thereby ensuring their mutual phase coherence. Recall that the beam splitters labeled with η are only shown to model losses in the detection—they are not present in the actual setup since detectors in the real world are inevitably imperfect.

Now that we have the probabilities of (no-)detection for each of the three modes, we can select what projection we want based on the experimental "recipe" we devised in Sec. II. We summarize it here:

$$\begin{aligned} &z \text{ basis: } t = 1, \quad n \geqslant 1 \quad \text{for} \quad z^+, \quad n = 0 \quad \text{for} \quad z^- \\ &x \text{ basis: } t \to 1, \quad \beta = 1, \quad \theta = \pi \quad \text{for} \quad x^-, \\ &\qquad \theta = 0 \quad \text{for} \quad x^+, \quad n = 0. \end{aligned} \tag{16}$$

Assembling all four probabilities that enter in Eq. (3), we can evaluate numerically the middle term of the inequality, rescale the x-basis projection probabilities according to Eq. (8), and simulate the effect of errors in the experimental parameters. Bell tests are then expected to be conclusive only if the middle term of the inequality is outside the [0, 1] range predicted by local theories.

IV. RESULTS

Assuming for now that all other experimental errors are zero, the middle term of the inequality can be plotted as a function of quantum efficiency η^2, which we take—for the sake of simplicity—to be uniform for all three detectors (Fig. 4).

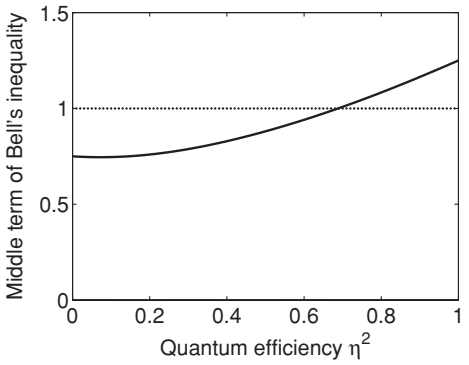

FIG. 4. Middle term of the tripartite Bell inequality as a function of quantum efficiency. The dotted line delimits the upper value for which the inequality is satisfied. The parameters t, β, and θ were all assumed to have their nominal values.

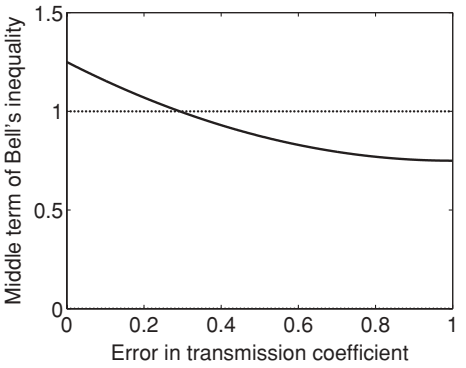

FIG. 5. Middle term of Bell's inequality as a function of the transmission coefficient t. All other parameters are ideal.

Making the fair sampling assumption, we see that in otherwise ideal conditions a minimum quantum efficiency of approximately 69% is required to violate local realism. Such a threshold is in the range of what photodetectors to date are capable of. Takeuchi *et al.* reported a 88% quantum efficiency Si shallow-impurity conduction-band detector [17], Billotta *et al.* measured quantum efficiencies up to 72% in Si single-photon avalanche diodes [18], and Rieke [19] quotes efficiencies of up to 98% for Si:As block impurity band (BIB) detectors with a reflective back surface.

Figure 4 assumes a W state as the input to the Bell measurement setup and we argued that this state can relatively simply be generated from a single photon state as explained in Fig. 3. A legitimate question is how to generate the single photon state. At present, the best way seems to be to first generate a photon pair through spontaneous parametric down-conversion (SPDC). The pairs are then produced randomly in time. However, it is possible to herald the space-time position of one of the photons if the other is detected at an auxiliary photodetector. The state of the remaining photon will then "collapse" to a single-photon state. A nonunity quantum efficiency of the heralding detector will not degrade the possible violation of the Bell inequality since, if the heralding photon is not recorded, one simply does not record anything from the three Bell measurement detectors in Fig. 3. Hence, a nonunity quantum efficiency of the heralding detector will simply reduce the rate of collecting data, but not degrade the data. On the other hand, dark counts in the heralding detector

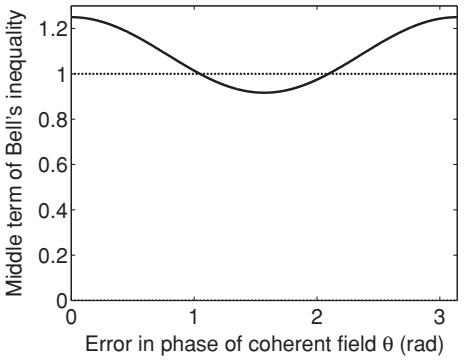

FIG. 6. Middle term of Bell's inequality as a function of the quantum phase θ of the coherent field. All other parameters are ideal.

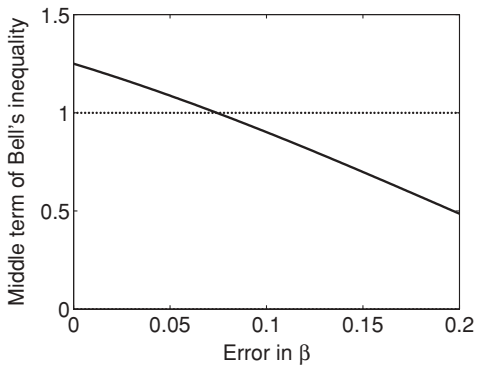

FIG. 7. Middle term of Bell's inequality as a function of β. All other parameters are ideal.

will trigger a recording from the three detectors although no photon was entering the setup, and such events, coming from the separable state $|0, 0, 0\rangle$, instead of the nonseparable W state, will reduce the middle term in Eq. (3). However, modern, good grade, solid state, Si avalanche photodetectors have dark count rates on the order of 25–100 Hz, whereas the photon-pair production rate can be in excess of 10^6 Hz [20]. Hence, the degradation of the middle term of Eq. (3) will be on the order of a factor $(10^6 - 100)/10^6 = 0.9999$, which is imperceptible within the resolution of Fig. 4.

Our result for high quantum efficiencies seems to confirm the findings in Ref. [8] where the authors conclude that the unbalanced homodyne measurements scheme used to measure along the x axis is actually relatively robust under photon loss (or equivalently, less than unity photodetector efficiency). This is in spite of the fact that one will assume relatively strict requirements in our case for two reasons. One is that while the bipartite Clauser-Horne-Shimony-Holt (CHSH) inequality (in the ideal case) can be violated by a factor $2\sqrt{2}/2 \approx 1.41$, the tripartite inequality (3) can only be violated by the factor 1.25, so that the margin of error is smaller already from the start. The second reason is that the inequality (3) requires the coincident detection of three independent detectors, so a deviation from an ideal characteristic of each detector will be multiplied by three in the final inequality while in a bipartite test of local realism the corresponding factor is two. The fact that a violation can still be detected with a detector whose quantum efficiency deviates substantially from unity makes the prospects of implementing the nonlocality test suggested in Ref. [4] realistic.

The introduction of experimental errors can also be simulated, with the predictable result that it will deteriorate the conclusiveness of the tests. Let us look at the effect of these experimental errors one at a time, taking all other parameters to be ideal. Consider, for example, an error Δt in the transmission coefficient that ranges from 0 to 1 (Fig. 5). At around $\Delta t \approx 0.3$, the middle term of Bell's inequality enters the zone where locality cannot be disproved. A similar situation arises for errors in the phase of the coherent state where $\Delta\theta \in [\pi/3, 2\pi/3]$ (Fig. 6). Indeed, if the quantum phase of the coherent field is off by $\pi/2$, beats between $|\psi_0\rangle$ and $|\alpha\rangle$ will be least likely to occur and in fact we are implementing a projection along the y axis rather than the x axis, thereby defeating our measurement scheme Of all errors in experimental parameters, $\Delta\beta$ is the one which the inequality is the most sensitive to (Fig. 7). This can be seen from the rapid descent of the middle term of the inequality into the "locality zone" starting at $\Delta\beta \approx 0.1$.

V. CONCLUSION

In brief, we built a mathematical model of a Bell inequality with a single-photon W state, which incorporates experimental parameters. The prime challenge to this end came from the fact that photon detection is the only measurement technique available and that it, *per se*, does not seem useful in performing measurements onto bases other than the photon number basis. To remedy this, we adopted an unbalanced homodyne measurement scheme, which acted as an approximate projector onto the x or y bases in Fock space. Our scheme seems easier and more realistic to implement experimentally than either of the two schemes proposed in Ref. [4].

Our scheme was subsequently shown to be valid for such projective measurements under the condition that we operate with quantum efficiencies reasonably close to unity. This scheme should be of value for general qubit measurements in the bases complementary to the photon number basis, which we have been taken to be the z basis. Hence, though we applied such projections to the particular case of the W state, they can be equally used for the characterization of any photonic qubits of the form $|\psi_0\rangle = \sqrt{p}|0\rangle + e^{i\Phi}\sqrt{1-p}|1\rangle$.

An expression for the middle term of the Bell inequality was obtained, which was then numerically analyzed to simulate the effect of experimental imperfections. The main result was that a quantum efficiency of at least 69% is required if any manifestation of nonlocality is to be shown with a W state in Fock space. Additionally, the middle term of Bell's inequality was graphed as a function of experimental errors, one parameter at a time, to visualize the effect of each imperfection on the conclusiveness of Bell tests. In relative terms, the second-most sensitive parameter after the detector efficiency is the beating-field amplitude $\beta = |\alpha|t$, which can only err by 10% or so. On the positive side, this parameter is easy to adjust experimentally since it only requires an adjustment of the coherent field amplitude $|\alpha|$.

ACKNOWLEDGMENTS

This work was supported by the Swedish Research Council (VR).

[1] *Quantum Unspeakables: From Bell to Quantum Information*, edited by R. A. Bertlmann and A. Zeilinger (Springer, New York, 2002).
[2] W. Dür, G. Vidal, and J. I. Cirac, Phys. Rev. A **62**, 062314 (2000).
[3] W. Dür, Phys. Rev. A **63**, 020303(R) (2001).
[4] L. Heaney, A. Cabello, M. F. Santos, and V. Vedral, e-print arXiv:0911.0770.
[5] M. Eibl, N. Kiesel, M. Bourennane, C. Kurtsiefer, and H. Weinfurter, Phys. Rev. Lett. **92**, 077901 (2004).
[6] H. Jeong and N. B. An, Phys. Rev. A **74**, 022104 (2006).

[7] A. Cabello, Phys. Rev. A **65**, 032108 (2002).
[8] M. Wieśniak and M. Żukowski, Phys. Lett. **A372**, 1783 (2008).
[9] S. A. Babichev, B. Brezger, and A. I. Lvovsky, Phys. Rev. Lett. **92**, 047903 (2004).
[10] J. H. Shapiro, H. P. Yuen, and J. A. Machado Mata, IEEE Trans. Inf. Theory **25**, 179 (1979).
[11] G. Björk, P. Jonsson, and L. L. Sánchez-Soto, Phys. Rev. A **64**, 042106 (2001).
[12] D. F. Walls and G. J. Milburn, *Quantum Optics* (Springer, New York, 1995).
[13] R. Loudon, *The Quantum Theory of Light* (Oxford University Press, Oxford, 2000).
[14] W. Vogel and D.-G. Welsch, *Quantum Optics* (Wiley, New York, 2006).
[15] B. Hessmo, P. Usachev, H. Heydari, and G. Björk, Phys. Rev. Lett. **92**, 180401 (2004).
[16] S. Stenholm and K.-A. Suominen, *Quantum Approach to Informatics* (Wiley Interscience, New York, 2005).
[17] S. Takeuchi, J. Kim, Y. Yamamoto, and H. H. Hogue, Appl. Phys. Lett. **74**, 1063 (1999).
[18] S. Billotta, M. Belluso, G. Bonanno, P. Bruno, A. Calí, S. Scuderi, and M. C. Timpanaro, Mem. Soc. Astronom. Italiana Suppl. **9**, 433 (2006).
[19] G. Rieke, *Detection of Light: From the Ultraviolet to Submillimeter* (Cambridge University Press, Cambridge, England, 2003).
[20] J. H. Shapiro and N. C. Wong, J. Opt. B: Quantum Semiclass. Opt. **2**, L1 (2000).